Journal of Experimental Nanoscience
Publication details, including instructions for authors and subscription information:
http://www.informaworld.com/smpp/title~content=t716100757

Synthesis of epoxy ferrite nanocomposites in supercritical carbon dioxide

M. G. H. Zaidi[a]; P. L. Sah[b]; S. Alam[c]; A. K. Rai[d]
[a] Supercritical Fluid Processing Laboratory, Department of Chemistry, G.B. Pant University of Agriculture & Technology, Pantnagar, India [b] Department of Mechanical Engineering, G.B. Pant University of Agriculture & Technology, Pantnagar, India [c] Polymer Division, Defense Material Stores Research Development & Establishment, Kanpur, India [d] Department of Physics, Allahabad University, Allahabad, India

To cite this Article Zaidi, M. G. H. , Sah, P. L. , Alam, S. and Rai, A. K.(2009) 'Synthesis of epoxy ferrite nanocomposites in supercritical carbon dioxide', Journal of Experimental Nanoscience, 4: 1, 55 — 66
To link to this Article: DOI: 10.1080/17458080802656515
URL: http://dx.doi.org/10.1080/17458080802656515

Journal of Experimental Nanoscience
Vol. 4, No. 1, March 2009, 55–66

Taylor & Francis
Taylor & Francis Group

Synthesis of epoxy ferrite nanocomposites in supercritical carbon dioxide

M.G.H. Zaidi[a]*, P.L. Sah[b], S. Alam[c] and A.K. Rai[d]

[a]*Supercritical Fluid Processing Laboratory, Department of Chemistry, G.B. Pant University of Agriculture & Technology, Pantnagar, India;* [b]*Department of Mechanical Engineering, G.B. Pant University of Agriculture & Technology, Pantnagar, India;* [c]*Polymer Division, Defense Material Stores Research Development & Establishment, Kanpur, India;* [d]*Department of Physics, Allahabad University, Allahabad, India*

(*Received 15 January 2008; final version received 28 November 2008*)

A series of epoxy ferrite nanocomposites (EFNCs) was synthesised through dispersing ferrite nanoparticles (5.0 phr, parts per hundred of resin) into diglycidylether of bisphenol A (0.1 mol) in supercritical carbon dioxide at $85 \pm 1^{\circ}$C, 1600 psi over 1 h followed by curing with triethylene tetramine (15 phr) at $40 \pm 1^{\circ}$C. For this purpose, ferrite nanoparticles were synthesised through size-controlled precipitation method. The size of ferrite nanoparticles was calculated through XRD and further verified through transmission electron microscopy. The synthesised EFNCs were characterised through UV-Vis, FT-IR, laser-induced breakdown spectra, X-ray diffraction, scanning electron microscopy and vibrational sample magnetometry. The results showed that, with the decrease in size, the concentration of ferrite nanoparticle in EFNCs was increased ranging 3.843–4.042 phr. This resulted in a substantial increase in the compression, tensile, impact strength and Rockwell hardness of EFNCs. The effect of particle size on wear behaviour of EFNCs was investigated at various combinations of hydraulic end load ranging 1.0–3.0 bar and disc speed 230 rpm, which showed that a decrease in the size of ferrite nanoparticles imparts a remarkable reduction in wear volume over epoxy composite. All such EFNCs showed super-paramagnetic behaviour with saturation magnetisation ranging 15.8–39.91 emu g^{-1}.

Keywords: epoxy ferrite nanocomposites; synthesis; supercritical carbon dioxide; spectral; morphological and mechanical properties; hysteresis

1. Introduction

Supercritical fluids, particularly supercritical carbon dioxide ($scCO_2$), have gained significant technological incentives over the past few decades due to their gas-like diffusivity and liquid-like density. The unique property of diffusion of $scCO_2$ increases the free volume and the mobility of the polymer chains with simultaneous reductions in the

*Corresponding author. Email: mgh_zaidi@yahoo.com

ISSN 1745–8080 print/ISSN 1745–8099 online

DOI: 10.1080/17458080802656515
http://www.informaworld.com

glass transition temperature and viscosity. This has opened opportunities to synthesise and process a variety of materials ranging from nanoparticles to polymer-based composites with enhanced mechanical, thermal and electrical properties [1–3].

Conventionally polymer-based nanocomposites are synthesised through either reactive or nonreactive routes in aqueous or organic phases. In this connection, ferrite nanoparticles of a wide range of sizes were impregnated into various polymer matrixes to produce their corresponding nanocomposites. A reactive route based on impregnation or *in situ* polymerisation for producing polymer-based nanocomposites involves polymerisation of monomers in the presence of an initiator in suitable solvent media to produce their corresponding nanocomposites. This route has been applied to synthesise nanocomposites through either dispersing ferrite nanoparticles into epoxy resin followed by curing of epoxy resin with amine functional hardeners [4,5] or *in situ* polymerisation of various vinyl functional monomers in the presence of free radical initiators in organic solvents [6–8]. A nonreactive route of synthesis of these nanocomposites involves infusion of magnetic nanoparticles into polymer matrix in the presence of suitable organic solvents. Through the nonreactive route a variety of magnetic nanoparticle-reinforced composites were synthesised using polypyrrole [9], styrene-divinylbenzene copolymer [10], urethane/urea elastomer [11], polyaniline containing polyethylene glycol as a surfactant [12], polyvinyl acetate [13], poly(methylmethacrylate) [14], amine functional polyglycidyl methacrylate [15], glycerol mono(meth)acrylate and their block copolymers [16,17], polyvinyl pyridine [18], and biocompatible polymers such as dextran as polymer matrix [19].

Realising the technological limitations related to the hazardous nature, recovery and disposal of organic solvents used as a medium of processing magnetic nanocomposites, we have recently used $scCO_2$ as an inexpensive and environmentally benign alternative medium to synthesise polyvinyl pyridine ferrite nanocomposite comprising enhanced ferrite content and saturation magnetisation [18]. A literature survey revealed that although synthesis of epoxy ferrite nanocomposites, their magnetic, morphological properties and X-ray fluorescence spectra have been investigated [4,5], no efforts have been made to synthesise the proposed epoxy ferrite nanocomposites (EFNCs) through reinforcing ferrite nanoparticles at different sizes into epoxy resin in $scCO_2$ and to study their detailed mechanical properties. In the present investigation, efforts have therefore been made to synthesise the proposed EFNCs comprising enhanced magnetic and mechanical properties through infusing ferrite nanoparticles comprising different sized at 5.0 phr(parts per hundred of resin) concentration into diglycidylether of bisphenol A (DGEBA, 0.1 mol) in $scCO_2$ at 1600 psi, $85 \pm 1^{\circ}C$ for 1.0 h followed by degassing and curing the treated epoxy with triethylene tetramine (TETA, 15 phr) at $40 \pm 1^{\circ}C$. The synthesised EFNCs were characterised through their spectra, morphology, magnetic, and mechanical properties with reference to an epoxy composite [Io], synthesised in the absence of ferrite nanoparticles under identical conditions [4,5,18–22]. The synthesised EFNCs may find their applications as microwave absorbing materials [23,24] and coating materials for on-chip bondwire inductors and transformers offering a cost-effective approach to realising power systems on chip. More importantly, such bondwire magnetic components have been reported to be easily integrated into systems on chip manufacturing processes with minimal changes and open enormous possibilities for realising cost-effective, high-current, high-efficiency power systems on chip [25].

2. Experimental

2.1. *Starting materials*

The commercially available diglycidyl ether of bisphenol-A (DGEBA) and triethylene tetramine (TETA) were purchased from Ms Cibatul India Ltd India. Epoxy equivalent of DGEBA (197 g Eq^{-1}) was deduced according to pyridinium chloride method [3]. Ferrite nanoparticles with size ranging 11–20 nm were synthesised through size-controlled precipitation method [8,18]. This method was based on optimizing two factors, namely; the concentration of precursor solution and the precipitation rate that controls the particle size. Briefly, a series of solutions of ferrous chloride ($FeCl_2 \cdot 4H_2O$) was prepared by dissolving their different quantities (3.0, 0.6 and 0.05 g) in double-distilled water (100 mL) under vigorous stirring. To this 50 mL of 7.0 molar ammonia solution (NH_4OH) was added dropwise at the rate of $\sim$0.33 mL s^{-1} with continuous stirring at $80 \pm 1^{\circ}C$. In the early stage of the reaction, brown precipitate was formed that was subsequently dried overnight in air at room temperature to provide the desired ferrite phase [18].

2.2. *Synthesis of EFNCs in $scCO_2$*

All EFNCs were synthesised in a stainless steel high-pressure reactor (100 cm^3), manufactured by Pressure Products Industries USA, equipped with PID temperature controller. The reactor was charged with a mixture composed of DGEBA (0.1 mol), ferrite nanoparticle (5.0 phr) and requisite amount of carbon dioxide. The contents were heated at 1600 psi, $85 \pm 1^{\circ}C$ for 1.0 h in $scCO_2$. The cell was cooled to $40 \pm 1^{\circ}C$ and the CO_2 was vented into dichloromethane. The cell was opened to give epoxy/ferrite formulations that were further degassed at $40 \pm 1^{\circ}C$, cured with TETA (15 phr) and fabricated into required dimensions (IS 1708) for evaluation of their mechanical properties with reference to an epoxy composite [Io] synthesised in the absence of ferrite nanoparticles under identical supercritical conditions (Table 1).

3. Measurements

Ultraviolet-visible spectra were recorded on a Genesis 10 thermo Spectronic spectrophotometer in chloroform. FT-IR spectra were recorded on a Bucker FT-IR

Table 1. Magnetisation and mechanical properties of EFNCs.

		EFNCs		
Properties	[Io]	[I]	[II]	[III]
Size of ferrite [XRD (TEM)] (nm)		20.0(20.50)	17.0(18.30)	11.0(10.60)
Ferrite content (phr)	–	3.843	3.912	4.042
Saturation magnetisation (emu g^{-1})	–	15.8	29.7	39.91
Compressive strength $\times 10^4$ (N m^{-2})	1565.12	1544.52	1820.08	1857.75
Charpy impact strength (Nm)	61.78	64.23	73.55	85.02
Tensile strength $\times 10^4$ (Kg cm^{-2})	2506.54	1283.47	1713.29	1743.79
Rockwell hardness (RH scale)	157.33	182.0	178.33	176.0

Spectrophotometer in KBr. An X-ray powder diffraction (XRD) pattern of samples was recorded at 25°C over a Rigaku-Geigerflex diffractometer using Cu–Kα radiation ($\lambda = 0.154056$). The size of ferrite nanoparticles was calculated through XRD and further verified through TEM. The XRD peaks were observed at 2θ and the corresponding *hkl* values were calculated. The unit cell volume and particle size of corresponding ferrite nanoparticles were calculated using the Debye–Scherrer equation. The concentration of ferrite nanoparticles (phr) in EFNCs was determined with slight modification of the method reported earlier [18]. In brief, EFNC (5.0 g) was dissolved in sulphuric acid (sp.gr.1.84, 50 mL) and aliquot (5 mL) of this solution was mixed with freshly prepared sodium tartarate (5%, 10 mL) and 1,10-phenanthroline monohydrochloride (2%, 10 mL). The volume of content was raised to 100 mL, then the optical density of resulting solution was measured at $\lambda_{max} = 516$ nm by UV-Vis spectrophotometer. In order to determine the concentration of iron in the solutions, a calibration curve was plotted from a set of standard solutions at different Fe^{3+} concentrations. The concentration of Fe^{3+} in EFNCs was deduced from their respective optical density (OD) using linear equation: $OD = (-0.077 + 7.86n_{Fe+3})$, where, n is the concentration of Fe^{+3} (ppm). The volume concentration of Fe ($\varphi_{Fe+3} = V_{Fe}/V_{solution}$) was converted to the ferrite concentration as phr ($\varphi = V_{ferrite}/V_{solution}) \times 10^2$ using the formula $\varphi = k\varphi_{Fe+3}$ [18]. The laser-induced breakdown spectra (LIBS) of ferrite nanoparticle, epoxy resin [Io] and corresponding EFNCs were recorded by using a Q-switched Nd:YAG laser (Continuum Surelite III-10, USA) emitting at 1064 mm, with 28 ns pulse duration and a LIBS 2000^+ spectrometer (Ocean Optics, USA) equipped with CCD. LIBS is a well-established, sensitive method to perform rapid elemental analysis of various materials irrespective of their physical states. In the present method, an intense laser pulse was focused on the surface of a material that ablated a small quantity and produced a plasma plume above the surface. The ablated material was vaporised and then partly atomised, excited and ionised. The excited atoms and ions in the plasma emitted a secondary light, which was collected and spectrally resolved by a spectrophotometer and analysed by a light detector. The emission spectrum from the plasma plume was detected and used for identification of the elements present in the ablated material. The method offers a number of advantages of considerable importance. In particular, the sample does not have to be prepared, and a small amount of ablated material is sufficient [20]. The magnetic properties of EFNCs were studied using a vibrating-sample magnetometer VSM, EG&G Princeton Applied Research Vibrating Sample Magnetometer, model 155 at room temperature [13,14,22]. TEM of ferrite samples were recorded over JEOL 1011 (Tokyo, Japan) with a primary beam voltage of 80 kV. Electron micrographs of gold coated, longitudinal sections of samples were scanned at 1000× magnifications over LEO-435 [4,5,18,19,21,22].

The compression strength ($\times 10^4$ N m^{-2}) of the samples was recorded on a Tinus Olson universal testing machine (UTM). The Charpy Impact Strength (Nm) of EFNCs was directly recorded on a UTM as energy required inducing a visible crack. The tensile strength ($\times 10^4$ kg cm^{-2}) of specimens was directly recorded on the dial gauge of a Instron Universal Testing Machine at the test specimen gauge length 55 mm, diameter 20 mm, total shoulder length 200 mm and end diameter 25 mm. The Rockwell hardness of the specimen was recorded in terms of R scale over hardness testing machine with ball indenter (½″, 12.70 mm) at the minor load of 10 kg (Table 1). The wear behaviour of EFNCs was studied at different combinations of hydraulic end load ranging 1.0–3.0 bar at disc speed

230 rpm was studied over pin on disc machine TE- 97/7050 (750 W, three phase) with 14 spindle speeds ranging 25–2150 rpm and fitted with Muyford super lathe, dead weight tester, and transducer with calibration 0.892 mv v^{-1}.

4. Results and discussion

Epoxy ferrite nanocomposites comprising ferrite nanoparticles of different sizes were synthesised through dispersing ferrite nanoparticles (5.0 phr) into diglycidylether of bisphenol A (0.1 mol) at 1600 psi, $85 \pm 1^{\circ}C$ for 1 h in $scCO_2$. The contents were degassed and cured with TETA (15 phr) at $40 \pm 1^{\circ}C$. This has afforded corresponding EFNCs [I–III] comprising volume concentration (phr) of ferrite nanoparticles ranging 3.843–4.0442. The formation of EFNCs [I–III] was ascertained through UV-Vis, FT-IR, LIBS, and scanning electron microscopy. The size of ferrite nanoparticles was calculated through XRD using Debye–Scherer equation and further verified through TEM. The effect of volume concentration and size of ferrite nanoparticles on the morphology, mechanical and magnetic properties of corresponding EFNCs [I–III] was investigated.

In order to get an insight into the affinity of ferrite nanoparticles with epoxy resin the UV-Vis and FT-IR spectra of EFNC [III] were studied. The curing agent (TETA) has shown absorption at 287 nm. Curing of DGEBA with TETA result [Io] comprising a pair of auxochromes as –OH and –NH–. This has blue shifted the absorption of DGEBA from 257 to 230 nm corresponding to [Io] due to π–π^* transition [3]. Ferrite has shown a pair of strong absorptions at 209 nm and a weak absorption at 257 nm. The corresponding nanocomposite [III] has also shown a strong absorption at 221 nm and a weak absorption at 251 nm respectively. Such a shift in absorption of [III] over ferrite may be due to n–π^* transition (Figure 1). A FT-IR spectrum has also reflected the formation of –OH group due to condensation of amino group of TETA with epoxy group of DGEBA. The composite [Io] has shown a wide band at 3426.66 cm^{-1} corresponding to ν_{O-H} that was shifted to lower frequency at 3490.66 cm^{-1} due to the existence of intermolecular hydrogen-bonded –OH groups. A shift of ν_{O-H} from the standard data (3550–3200 cm^{-1}) to 3426.66 by 123.34 cm^{-1} corresponds to medium level intramolecular hydrogen bonding in [Io], formed between the adjacent –OH and –NH groups [21]. The corresponding EFNC [III] has shown stretching band corresponding to the coordination of ferrite nanoparticles with –OH and $–NH_2$ groups of cured resin at 668.9 and 586.4 cm^{-1} respectively (Figure 2) [18].

Figure 3(a) shows a representative XRD spectrum of ferrite nanoparticle. XRD patterns show a large amorphous zone as well as typical peaks, which can be attributed to a nanocrystalline magnetite (Fe_3O_4) or maghemite (γ-Fe_2O_3).The XRD measurement, revealed peak characteristics of ferrite at $2\theta = 2.9408$, 2.5081, 2.0870 with *hkl* values (220), (311), (400). The peaks indexed to (220), (311), (222), (400), (422), (511), and (440) planes of a cubic unit cell, correspond to that of ferrite structure. X-ray peaks show excellent agreement, in peak position and relative intensity, with the ASTM data [7]. Debye–Scherrer calculations provided the corresponding size of ferrite nanoparticles ranging 11–20 nm [22]. After close examination the presence of two distinct phases is excluded and the composition is thought to consist of a defective magnetite structure with a lattice parameter in between the one of bulk magnetite and bulk maghemite. The corresponding nanocomposites have shown a greater extent of amorphous zone with peaks identical to ferrite nanoparticles indicating intact crystalline nature in each of the

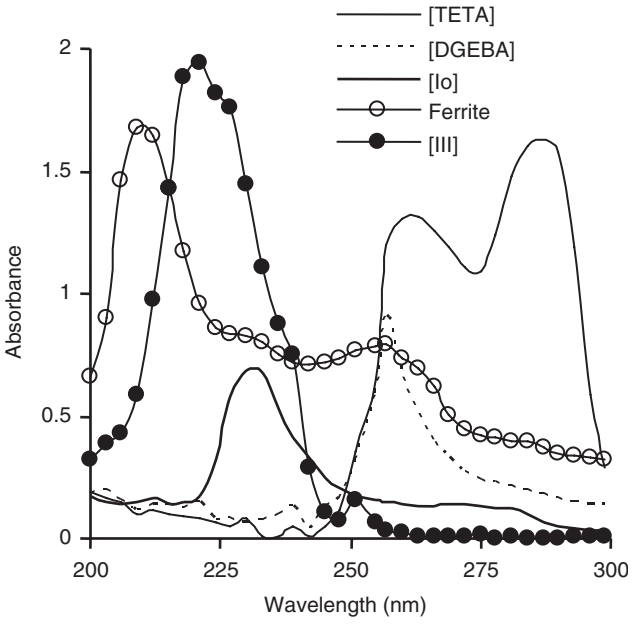

Figure 1. UV-Vis spectra.

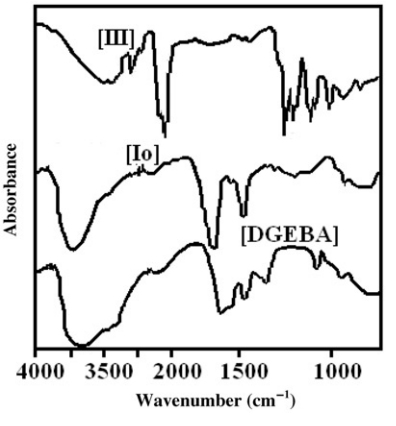

Figure 2. FT-IR spectra.

EFNCs (Figure 3(b) and (c)). The TEM images and respective particle size distribution of ferrite nanoparticles has been shown in Figure 4(a)–(c). TEM data clearly indicate that the size of ferrite nanoparticles was in agreement with XRD data (Table 1).

Figure 5 represents the unique spectral signatures of each element present in epoxy composite [Io], ferrite and corresponding EFNC [III] in their LIBS. The epoxy composite [Io] has shown atomic lines corresponding to C(II) at 283.336, 427.347, 722.609, O(I) 777.366, O(II) at 396.663, N(I) at 747.185, N(II) at 399.875, 445.20, 462.552, 500.688 and

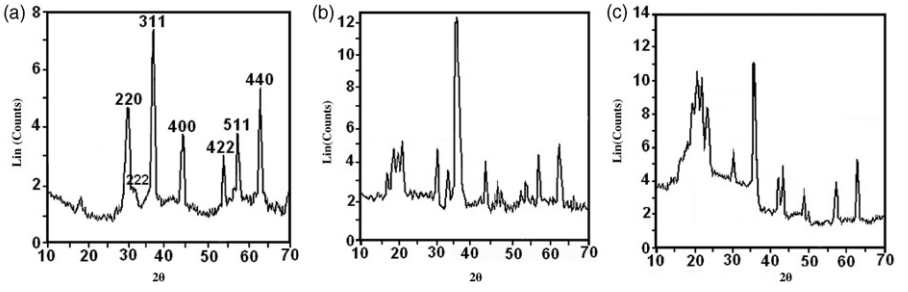

Figure 3. XRD spectrum of (a) ferrite nanoparticle, (b) EFNC[I], (c) EFNC [III].

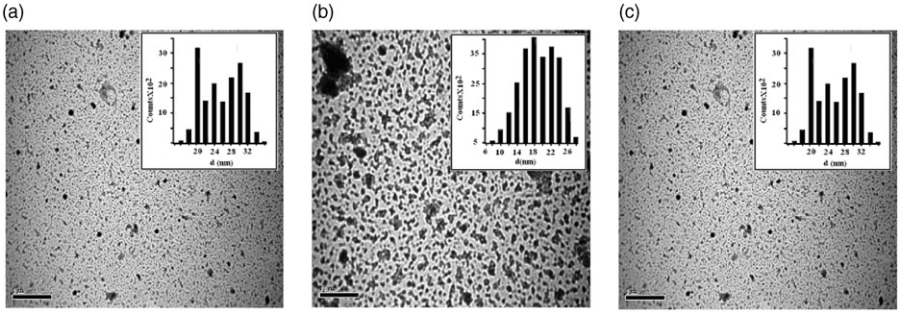

Figure 4. Transmission electron micrographs with inscribed particle size distribution histograms of ferrite nanoparticles: (a) 20.50 nm, (b) 18.30 nm, (c) 10.60 nm.

H(α) 486.133, H(β) at 656.331. Characteristic atomic lines corresponding to ferrite were observed for Fe (II) at 234.748, 240.369, 344.589, 358.447, 373.662, 381.949, 386.089, 404.924, 438.347, 623.411 respectively. Atomic lines corresponding to [III] were observed for C(II) at 283.804, 427.374, 229.592, O(II) at 777.792, O(II) at 396.66, N(II) at 445.197, 500.688, H(α) 486.133, H(β) at 658.331, Fe(III) at 271.681, 358.448, 373.662, 381.949, 386.089, 404.465, 438.347, 438.347 and Fe(II) at 234.279, 240.369, 274.479 respectively. Ferrite and corresponding EFNC [III] indicated common atomic lines corresponding to Fe(III) at 234.748, 249.26, 344.589, and 623.411. The absorption corresponding to Fe(II) at 238.827 and 260.945 in ferrite disappeared in EFNC [III]. The absorption corresponding to N(I) at 747.188 and N(II) at 399.875 for [Io] was eliminated in EFNC [III]. Further, EFNC [III] has shown additional new absorptions corresponding to Fe(II) at 248.792 and Fe(III) at 271.681 that support the formation of nanocomposite. LIBS of epoxy composite [Io] and EFNC [III] clearly show the atomic lines for C(II) 229.564 and 247.786 nm, N(III) at 868.395 nm and these lines are distinctly absent in the LIBS of ferrite. In contrast to this, large numbers of atomic lines of Fe are present in LIBS of ferrite as well as in composite material, while these lines are clearly absent in the LIBS of epoxy composite [Io]. The atomic lines of H(I) at 656.331 nm and O(II) at 777.362 nm are present in the LIBS of all three samples but the intensity of H lines is very weak in the LIBS of ferrite. The presence of weaker atomic lines of H in the LIBS of ferrite is probably due to moisture content in ferrite. Similarly, the presence of atomic line corresponding to oxygen

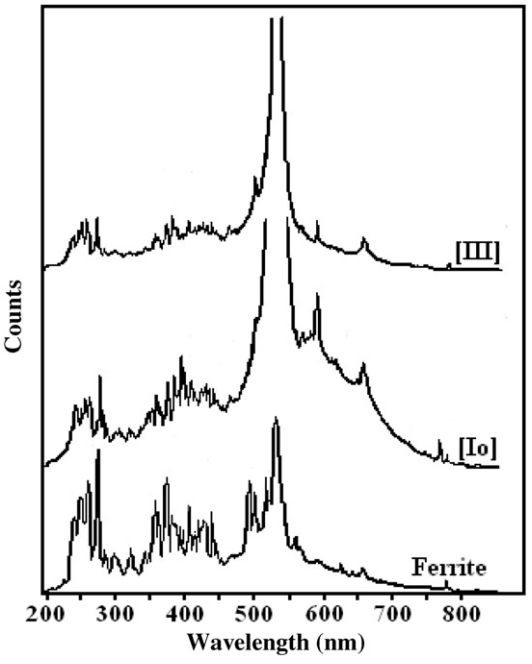

Figure 5. Laser-induced breakdown spectra.

may also be due to moisture content in [Io]. These spectral results clearly demonstrate the chelation of epoxy composite [Io] through nitrogen atom with ferrite to result the corresponding EFNCs [18,22].

The electron micrographs clearly indicate phase-separated morphology of cured epoxy resin [Io]. All EFNCs nanocomposites have shown nonuniform distribution of ferrite nanoparticles into epoxy matrix (Figure 6(a)–(d)). A regular increase in the phase separation in EFNCs was observed with size of ferrite nanoparticles (Figure 6(b)–(d)). At highest size the corresponding EFNC [III] has shown agglomerated ferrite nanoparticles into epoxy matrix (Figure 6(d)).

Figure 7 shows variations in magnetisation *versus* applied magnetic field for EFNCs comprising ferrite nanoparticles with various sizes. The nature of the hysteresis curves and the corresponding values of saturation magnetisation (emu g^{-1}) of EFNCs were dependent on the size of ferrite nanoparticles [18,22]. With the decrease in the size of ferrite nanoparticles, the corresponding EFNCs have shown increasing saturation magnetisation (Table 1). For example, EFNC [I] has shown a smooth hysteresis curve with saturation magnetisation 39.91 emu g^{-1}. A slightly irregular hysteresis curve with saturation magnetisation 29.7 emu g^{-1} was observed for EFNC [II]. Finally, the EFNC [III] has shown irregular hysteresis curve with saturation magnetisation 15.8 emu g^{-1}. In addition, the magnetisation decreases from the plateau value and reaches zero (i.e., no remanence effect) when the magnetic field intensity decreases, indicating the superparamagnetic properties of EFNCs. The behaviour shows that the iron oxide nanoparticles correspond to a single crystal domain exhibiting only on orientation of the magnetic moment and magnetite in structure (Figure 7).

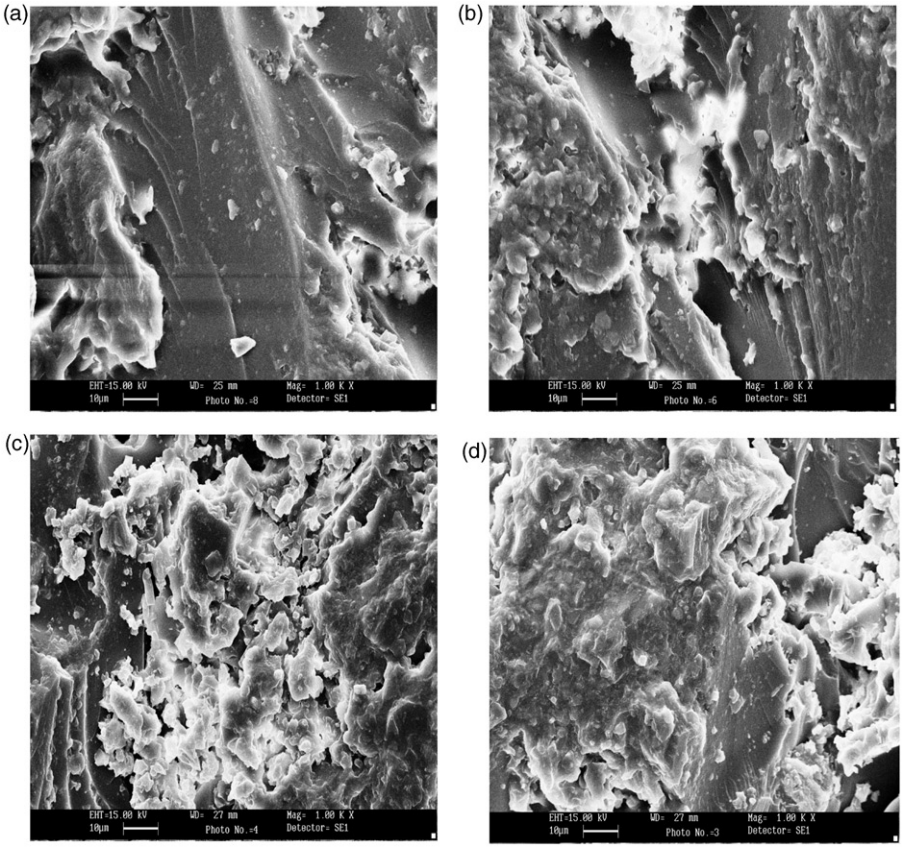

Figure 6. Scanning electron micrographs at 1000×: (a) [Io], (b) [I], (c) [II], (d) [III].

A regular increase in mechanical properties of EFNCs was observed with the decrease in the size of ferrite nanoparticles. The [Io] has shown compressive strength ($\times 10^4\,\mathrm{N\,m^2}$) at 1565.12. The EFNC [III] has shown highest level of compressive strength at 1857.75, followed by 1820.08 for EFNC [II] and 1544.52 for EFNC [I]. The composite [Io] has shown Charpy impact strength (Nm) at 61.78. This was increased to 85.02 corresponding to EFNC [III]. Charpy impact strength corresponding to EFNC [II] was observed as 73.54. This was further reduced to 64.23, corresponding to EFNC [III]. All the EFNCs showed lower tensile strength ($\times 10^4\,\mathrm{kg\,m^{-2}}$) over the epoxy composite [Io]. With the increase in the size of the ferrite nanoparticles, the tensile strength of corresponding EFNCs was also increased ranging 1283.47–1743.79 (Table 1). The wear behaviour of EFNCs [I] and [III] was studied and compared with reference epoxy composite [Io] at various hydraulic end load ranging 1.0–3.0 bar at disc speed 230 rpm (Figure 8). All EFNCs showed nonuniform wear behaviour at various combinations of hydraulic end load and disc speeds. The composite [Io] has shown highest wear volume 5.99 $\mathrm{mm^3}$ at 3 bar within 180 min. Under the similar conditions, the EFNCs [I] and [III] showed a remarkable decrease in wear volume at 4.12 and 4.58 $\mathrm{mm^3}$ respectively [3].

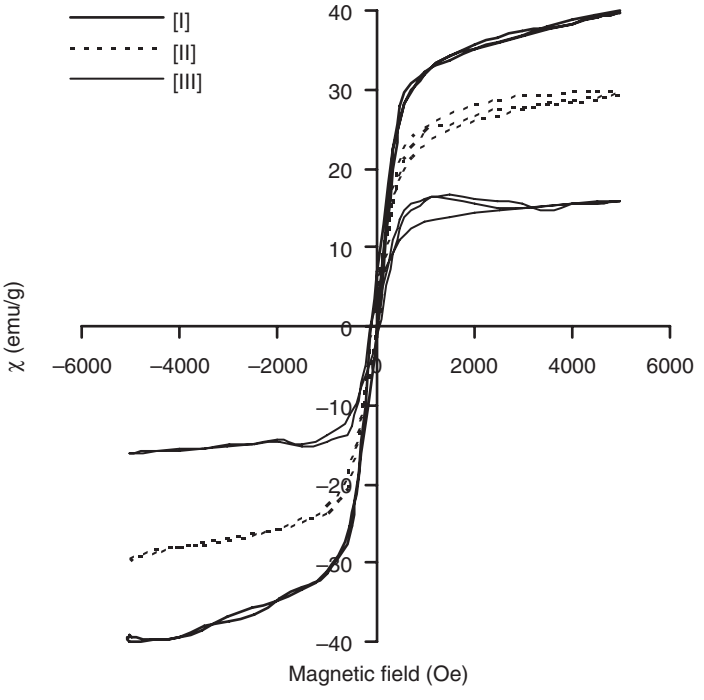

Figure 7. Effect of particle size of ferrite on magnetic susceptibility of EFNCs.

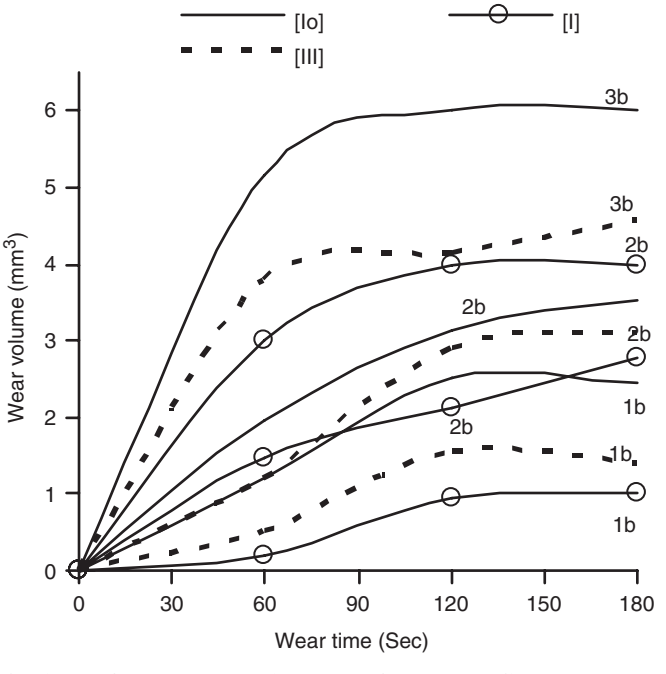

Figure 8. Wear behaviour of epoxy composite [Io] and corresponding EFNCs [I] and [III].

5. Conclusion

Epoxy ferrite nanocomposites (EFNCs) comprising ferrite nanoparticles with different size were synthesised through dispersing ferrite nanoparticles (5.0 phr) into diglycidylether of bisphenol A (0.1 mol) in supercritical carbon dioxide at 1600 psi over 1 h followed by curing with triethylene tetramine (15 phr) at $40 \pm 1^{\circ}C$. The presence of ferrite nanoparticles into epoxy matrix was ascertained through UV-Vis, FT-IR, LIBS, XRD and vibration sample magnetometry. The size of ferrite nanoparticles calculated from Debye–Scherrer equation was in agreement with transmission electron microscopy. Spectral analysis indicates the bonding of ferrite nanoparticles with epoxy matrix. XRD patterns clearly indicate identical crystal structure of the ferrite nanoparticles with intact crystalline nature in each of the EFNCs. The size of ferrite nanoparticles has greatly influenced the morphology, magnetic behaviour and mechanical properties of corresponding EFNCs. With decrease in the size of ferrite nanoparticles, the corresponding EFNCs showed a regular increase in the saturation magnetisation, compression, tensile, impact strength, and Rockwell hardness. All EFNCs showed nonuniform wear behaviour. The wear behaviour of EFNCs was increased with the particle size of ferrite nanoparticles at all the combinations of hydraulic end load and disc speeds.

Acknowledgements

Financial support from the Research Grant No. ERIP/ER/0403449/M/01/2004 funded by Government of India is acknowledged.

References

[1] S.P. Nalawade, F. Picchioni, and L.P.B.M. Janssen, *Supercritical carbon dioxide as a green solvent for processing polymer melts: Processing aspects and applications*, Prog. Polym. Sci. 31 (2006), pp. 19–43.

[2] Q. Peng, Q. Xu, H. Xu, M. Pang, J. Li, and D. Sun, *Supercritical CO_2-assisted synthesis of poly (acrylic Acid)/Antheraea pernyi SF Blend*, J. Appl. Polym. Sci. 98 (2005), pp. 864–868.

[3] M.G.H. Zaidi, N. Bhullar, V.P. Singh, P.L. Sah, S. Alam, and R. Singh, *Mechanical and thermal properties of epoxy polymethyl methacrylate blends synthesized in supercritical carbon dioxide*, J. Appl. Polym. Sci. 103 (2007), pp. 1303–1310.

[4] M.S. Al-Haik, H. Garmestani, D.S. Li, M.Y. Hussaini, S.S. Sablin, and R. Tannenbaum, *Mechanical properties of magnetically oriented epoxy*, J. Polym. Sci. 42 (2003), pp. 1586–1600.

[5] A.N. Thorpe, F.E. Senftle, M. Holt, and J. Grant, *Magnetization, micro-X-ray fluorescence, and transmission electron microscopy studies of low concentrations of nanoscale Fe_3O_4 particles in epoxy resin*, J. Mater. Res. 15 (2000), pp. 2488–2493.

[6] H. Daniel and B. Nataliya, *Magnetic poly(glycidyl methacrylate) microspheres prepared by dispersion polymerization in the presence of electrostatically stabilized ferrofluids*, J. Polym. Sci. Part A: Polym. Chem. 42 (2004), pp. 5827–5837.

[7] Z.Z. Xu, C.C. Wang, W.L. Yang, Y.H. Deng, and S.K. Fu, *Encapsulation of nanosized magnetic iron oxide by polyacrylamide via inverse miniemulsion polymerization*, J. Magn. Magn. Mater. 277 (2003), pp. 136–143.

[8] I. Neamtu, A. Ioanid, and A. Chiriac, *Polymer-coated ferrite nanocomposites synthesized by plasma polymerization*, J. Phys. 50 (2004), pp. 1081–1087.

[9] R. Sharma, S. Lamba, and S. Annapoorni, *Magnetic properties of polypyrrole-coated iron oxide nanoparticles*, J. Phys. D: Appl.Phys. 38 (2005), pp. 3354–3359.
[10] P.C. Morais, E.C.D. Lima, D. Rabelo, A.C. Reis, and F. Pelegrini, *Magnetic Resonance of magnetite nanoparticles dispersed in mesoporous copolymer matrix*, J. Magn. Magn. Mater. 36 (2004), pp. 3038–3040.
[11] A.M.F. Neto, M.H. Godinho, T. Toth-Katona, and P. Palffy-Muhoray, *Optical, magnetic and dielectric properties of non-liquid crystalline elastomers doped with magnetic colloids*, Brazilian J. Phys. 35 (2005), pp. 184–189.
[12] R.F. Ziolo, *Self-stabilized aqueous ferrofluids: Properties and characteristics*, Eur. Cell Mater. 3 (2002), pp. 92–99.
[13] W. Voit, D.K. Kim, W. Zapka, M. Muhammed, and K.V. Rao, *Magnetic behavior of coated superparamagnetic iron oxide nanoparticles in ferrofluids*, Mat. Res. 676 (2003), p. 124.
[14] J.L. Wilson, P. Poddar, N.A. Frey, H. Srikanth, K. Mohomed, K.J.P. Harmon, S. Kotha, and J. Wachsmuth, *Synthesis and magnetic properties of polymer nanocomposites with embedded iron nanoparticles*, J. Appl. Phys. 95 (2004), pp. 1439–1443.
[15] M. Zhiya, G. Yueping, and L. Huizhou, *Synthesis and characterization of micron-sized monodisperse superparamagnetic polymer particles with amino groups*, J. Polym. Sci. Part A: Polym. Chem. 43 (2005), pp. 3433–3439.
[16] H. Daniel, B. Nataliya, and L. František, *Effect of the reaction parameters on the particle size in the dispersion polymerization of 2-hydroxyethyl and glycidyl methacrylate in the presence of a ferrofluid*, J. Polym. Sci. Part A: Polym. Chem. 41 (2003), pp. 1848–1863.
[17] A.F. Thünemann, D. Schütt, L. Kaufner, U. Pison, and H. Möhwald, *Maghemite nanoparticles protectively coated with poly(ethylene imine) and poly(ethylene oxide)-block-poly(glutamic acid)*, Langmuir 22 (2006), pp. 2351–2357.
[18] M.G.H. Zaidi, N. Bhullar, D. Sharma, V. Agarwal, S. Alam, A.K. Rai and R.P. Pant, *Synthesis of polyvinyl pyridine ferrite nanocomposites in supercritical carbon dioxide*, J. Nanostr. Polym. Nanocomp. (2007), accepted.
[19] N. Tomašovičová, M. Koneracká, P. Kopčanský, M. Timko, and V. Závišová, *Infrared study of biocompatible magnetic nanoparticles*, Mesurement Sci. Rev. 6(2) (2006).
[20] R. Sattmann, I. Monch, H. Krause, R. Noll, S. Couris, A. Hatziapostolou, A. Mavromanolakis, C. Fotakis, E. Larrauri, and R. Miguel, *Laser-Induced Breakdown Spectroscopy for polymer dentification*, Appl. Spectrosc. 52 (1998), pp. 456–461.
[21] R.M. Silverstein and F.X. Webster, *Spectrophotometric Identification of Organic Compounds*, 6th ed., John Wiley & Sons Inc., New York, 1998, p. 87, chap. 3.
[22] S. Lee, J. Jeong, S. Shin, J. Kim, Y. Chang, K. Lee, and J. Kim, *Magnetic enhancement of iron oxide nanoparticles encapsulated with poly(d,l-latide-co-glycolide)*, Colloids and Surfaces A: Physicochem. Eng. Aspects 255 (2005), pp. 19–25.
[23] S.S. Kim, G.M. Cheong, and B.I. Yoon, *Ferrite-epoxy absorber on carbon fiber composite substrate*, J. Phys. IV France 07 (1997), C1-425-C1-426. DOI: 10.1051/jp4:19971172.
[24] A. Jänis, R.T. Olsson, S.J. Savage, U.W. Gedde, and U. Klement, *Microwave absorbing properties of ferrite based nanocomposites*, Proceedings of the SPIE 6526 (2007), 65261P.
[25] J. Lu, H. Jia, A. Arias, X. Gong, and Z.J. Shen, *On-chip bondwire magnetics with ferrite-epoxy glob coating for power systems on chip*, Int. J. Power Manage. Electron. 1 (2008), pp. 1–9.